Mar Geophys Res (2014) 35:69–85
DOI 10.1007/s11001-013-9210-8

ORIGINAL RESEARCH PAPER

Late Pleistocene–Holocene evolution of the southern Marmara shelf and sub-basins: middle strand of the North Anatolian fault, southern Marmara Sea, Turkey

Denizhan Vardar · Kurultay Öztürk · Cenk Yaltırak · Bedri Alpar · Hüseyin Tur

Received: 2 September 2013 / Accepted: 30 December 2013 / Published online: 10 January 2014

Abstract Although there are many research studies on the northern and southern branches of the North Anatolian fault, cutting through the deep basins of the Sea of Marmara in the north and creating a series of pull-apart basins on the southern mainland, little data is available about the geometrical and kinematical characteristics of the middle strand of the North Anatolian fault. The first detailed geometry of the middle strand of the North Anatolian fault along the southern Marmara shelf, including the Gemlik and Bandırma Bay, will be given in this study, by a combined interpretation of different seismic data sets. The characteristic features of its segments and their importance on the paleogeographic evolution of the southern shelf sub-basins were defined. The longest one of these faults, the Armutlu-Bandırma segment, is a 75-km long dextral strike-slip fault which connects the W–E trending Gençali segment in the east and NE–SW trending Kapıdağ-Edincik segment in the west. In this context, the Gemlik Bay opened as a pull-apart basin under the control of the middle strand whilst a new fault segment developed during the late Pleistocene, cutting through the eastern rim of the bay. In this region, a delta front forming the paleoshoreline of the Gemlik paleolake was cut and shifted approximately 60 ± 5 m by the new segment. The same offset on this fault was also measured on a natural scarp of acoustic basement to the west and integrated with this paleoshoreline forming the slightly descending topset–foreset reflections of the delta front. Therefore the new segment is believed to be active at least for the last 30,000 years. The annual lateral slip rate representing this period of time will be 2 mm, which is quite consistent with modern GPS measurements. Towards the west, the Bandırma Bay is a rectangular transpressional basin whilst the Erdek Bay is a passive basin under the control of NW–SE trending faults. When the water level of the paleo-Marmara lake dropped down to −90 m, the water levels of the suspended paleolakes of Bandırma and Gemlik on the southern shelf were −50.3 (−3.3 Global Isostatic Adjustment—GIA) and −60.5 (−3.3 GIA) m below the present mean sea level, respectively. As of today a similar example can be seen between the Sea of Marmara and the shallow freshwater lakes of Manyas and Uluabat. Similarly, the paleolakes of Gemlik and Bandirma were affected by the water level fluctuations at different time periods, even though both lakes were isolated from the Sea of Marmara during the glacial periods.

Keywords Southern Marmara Sea · Middle strand of the North Anatolian fault · High resolution seismic reflection · Multibeam · Paleoshoreline

D. Vardar (✉) · K. Öztürk · B. Alpar
Institute of Marine Sciences and Management, Istanbul University, Vefa, 34116 Istanbul, Turkey
e-mail: denizhan@istanbul.edu.tr

C. Yaltırak
Department of Geological Engineering, Istanbul Technical University, Maslak, 34669 Istanbul, Turkey

H. Tur
Department of Geophysical Engineering, Istanbul University, Avcılar, 34850 Istanbul, Turkey

Introduction

The North Anatolian fault (NAF) is a 1,500-km-long intracontinental transform fault (Şengör 1979) and splits into three branches (Barka and Kadinsky-Cade 1988) at the eastern part of the Sea of Marmara (Fig. 1). These branches

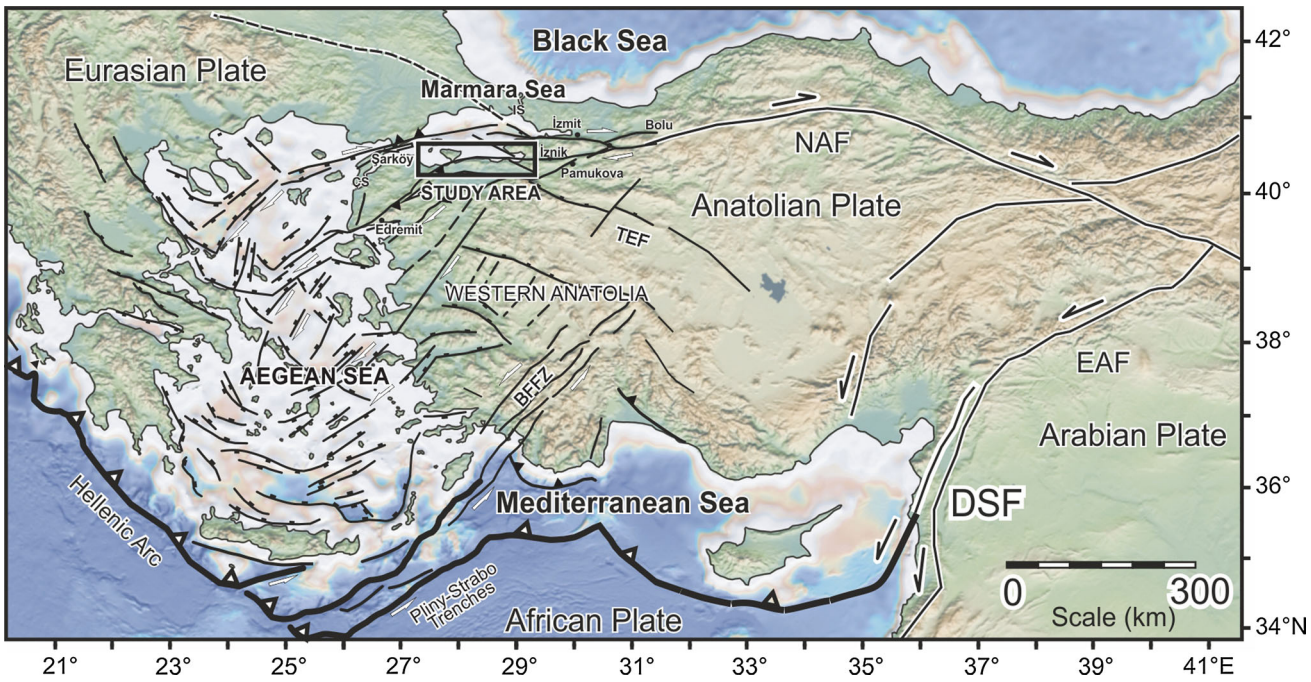

Fig. 1 Location map of the study area (Yaltirak et al. 2012). *NAF* North Anatolian fault, *TEF* Thrace-Eskişehir fault, *EAF* East Anatolian fault, *BFFZ* Burdur Fethiye fault zone, *DSF* Dead Sea fault, *IS* Istanbul strait, *CS* Canakkale strait

terminate against the normal faults at the northern Aegean Sea where the westward escape of the Anatolian block turns into anticlockwise rotational wedges (Yaltırak et al. 2012). All branches demonstrate different kinematic and seismic appearance in the region. Starting from east to west, the NAF bifurcates at the western side of 30.5°E longitude (Fig. 1). The northern strand extends from the city of Bolu to Izmit (Şengör 1979). Then the southern strand bifurcates in the Pamukova plain (Koçyiğit 1988). Its northern segment, known as the middle strand of the NAF (hereafter termed NAFMS), extends westward along the Lake Iznik (Öztürk et al. 2009), the Gemlik Bay (Yaltırak and Alpar 2002a), southern coast of the Bandırma Bay and then changes its direction by turning southwestward at the eastern part of the Erdek Bay. Meanwhile the southern strand of the NAF extends from the Pamukova plain towards the Gulf of Edremit in the west (Fig. 1; Yaltırak 2002).

Many studies have been devoted to the northern and southern branches, which cut through the deep basins of the Sea of Marmara in the north and create the Yenişehir pull-apart basin and the lakes of Uluabat and Manyas (Yaltırak 2002; Selim et al. 2013) in the south, respectively. However the geometry of the NAFMS under the sea and its kinematic features, which are less active if compared to the northern strand, have not been precisely studied previously.

The studies on the NAFMS have been mostly focused on the faults in the Gemlik Bay and partly its western approaches (Barka and Kadinsky-Cade 1988; Barka and Kuşçu 1996; Ergin et al. 1997; Alpar and Çizmeci 1999; Aksu et al. 1999, 2000; Yaltırak 2002; Yaltırak and Alpar 2002a; Adatepe et al. 2002; Gürer et al. 2003; Kurtuluş and Canbay 2007; Kuşçu et al. 2009). This basin was first considered as a pull-apart system (Barka and Kadinsky-Cade 1988; Barka and Kuşçu 1996; Fig. 2a). The basin developed during the Late Pliocene–Early Pleistocene (Yaltırak and Alpar 2002a), and is mainly controlled by west-trending dextral strike-slip faults aligned along the middle strand of the NAF zone (Fig. 2b). These faults cut the northwest-trending normal faults of the Thrace-Eskisehir Fault system (Fig. 1), which existed well before the east-trending main strike-slip faults. The southern shelf was uplifted tectonically due to the bending of the NAFMS in Bandırma Bay (Fig. 2c) and eroded starting from the Late Pliocene (Adatepe et al. 2002). On the basis of extensive high-resolution shallow seismic survey, Kuşçu et al. (2009) outlined four major fault zones in the Gemlik Bay, which are thought to be responsible for the formation of Burgaz pull-apart basin and so-called Gemlik push-up structure (Fig. 2d).

For Bandırma Bay, the only available seismic data (Kavukçu 1990) indicated that the seabottom was divided by NE–SW and E–W trending faults (Fig. 2d), indicating an inward collapse which is still active.

In this context the depression fields of the Gemlik Bay, including the Lake Iznik to the east (Öztürk et al. 2009), and the Bandırma Bay were developed on the transtensional regions between the fault segments that evolved during Late

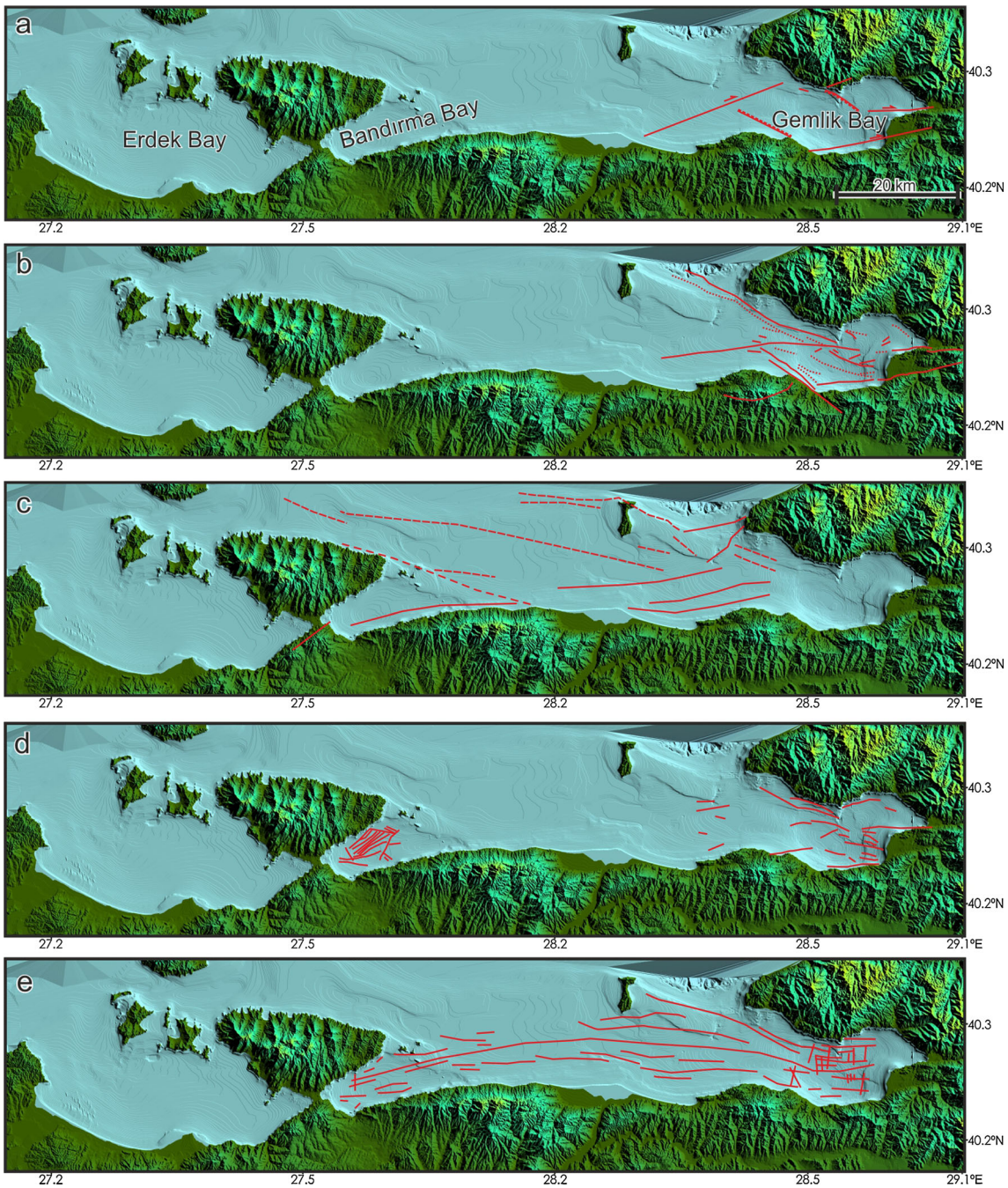

Fig. 2 Previous models proposed for the southern Marmara Sea; **a** pull-apart model based largely on morphology and bathymetry (Barka and Kuşçu 1996), **b** west-trending dextral strike-slip faults cutting the Thrace-Eskisehir fault system (Yaltırak and Alpar 2002a), **c** the faults causing tectonical uplift along southern shelf (Adatepe et al. 2002), **d** an inward collapse in the Bandırma Bay which is still active (Kavukçu 1990) and major fault zones in the Gemlik Bay responsible for the formation of Gemlik push-up structure (Kusçu et al. 2009), **e** a main fault model which has a lazy-Z shape in the Gemlik Bay and extends to Bandırma Bay (Kurtuluş and Canbay 2007)

Pliocene–Early Pleistocene under the control of right lateral strike-slip faults along the NAFMS. Yaltırak (2002) defined three en-echelon right-lateral fault segments bending between the Gemlik and Bandırma Bay, which forms the NAFMS under the sea. The bending causes N30°E-trending tension in addition to the strike-slip motion. According to Kurtuluş and Canbay (2007), Gemlik Bay is controlled by the boundary faults, a number of inactive faults with normal components, as well as by other active faults cutting through the seafloor. The right-lateral strike-slip geometry

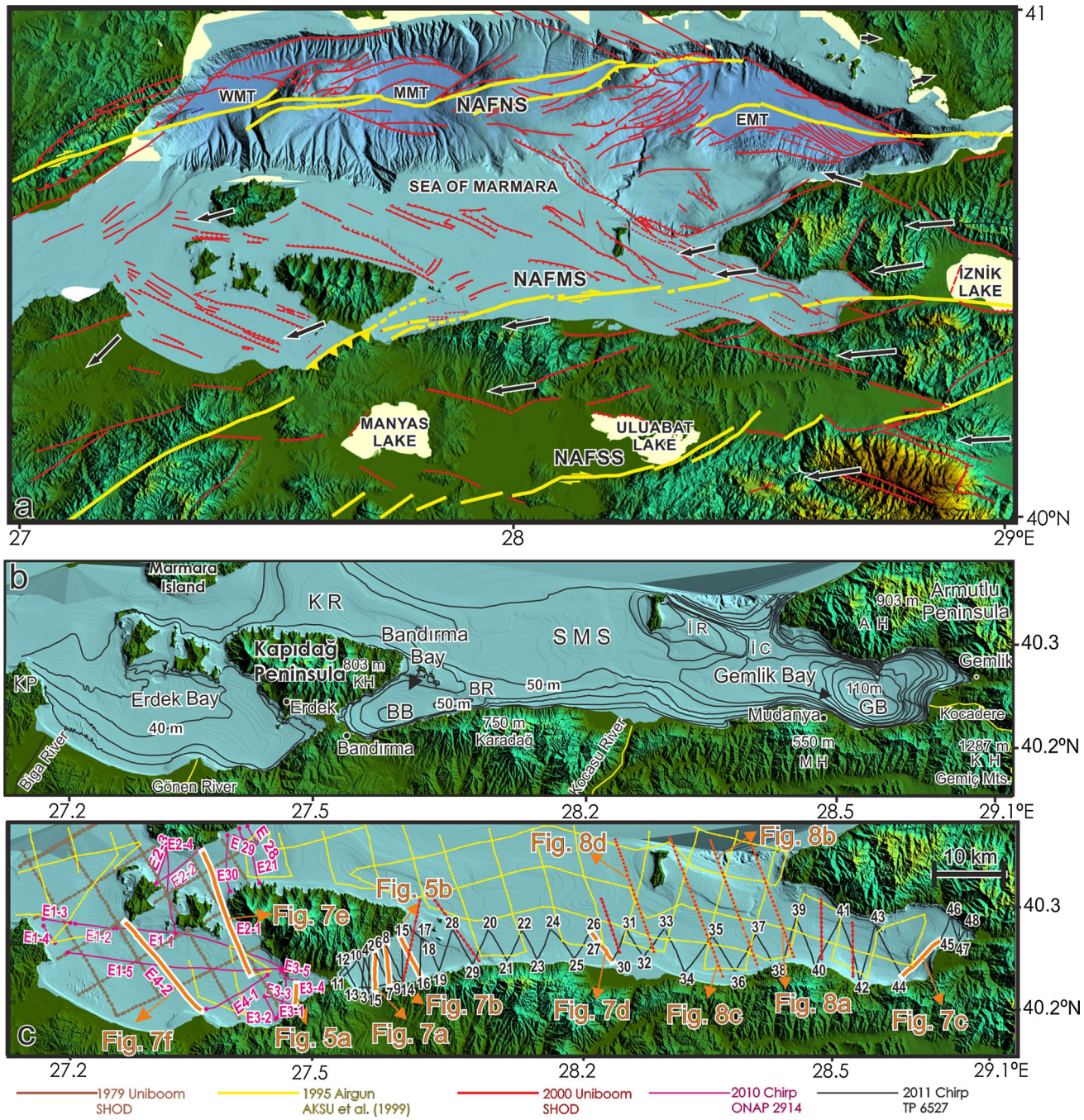

Fig. 3 **a** Fault map of the Sea of Marmara region after Yaltırak (2002). The faults along the southern margin of the Sea of Marmara were modified depending on our interpretation in this study. Multi-beam data of the Marmara deep basins and Tuzla region after Rangin et al. (2002) and Gökçeoglu et al. (2009), respectively. Arrows show the horizontal velocity field from Ergintav et al. (2007). *NAFNS* North Anatolian fault northern strand, *NAFMS* North Anatolian fault middle strand, *NAFSS* North Anatolian fault southern strand, *EMT* eastern Marmara trough, *MMT* middle Marmara trough, *WMT* western Marmara trough, **b** bathymetric and topographic features of the study area. *KP* Karabiga Promontory, *KH* Kapıdağ high, *KR* Kapıdağ ridge, *BB* Bandırma Basin, *SMS* South Marmara sill, *MH* Mudanya high, *IR* Imralı ridge, *IC* Imralı canyon, *AH* Armutlu high, *GB* Gemlik Basin, **c** location map of the seismic profiles

of NAFMS deformed the bay as a small "lazy Z-shaped" basin and Bandırma Bay as a "negative flower-structure" basin. The tectonic setting between these two sub-basins, on the other hand, was defined as pure strike-slip within an E–W trending fault system (Fig. 2e).

In the present paper we present new results from a shallow high-resolution Chirp seismic study carried out on the southern Marmara shelf, including the bays of Gemlik, Bandırma and Erdek. On the basis of the active faults observed on the seafloor and the morphological structures

on the seismic and multibeam data, we propose a new model explaining the Late Pleistocene–Holocene evolution of the middle strand of the NAF along the southern Marmara sub-basins and the paleogeographic development of the study area.

Physical setting of the study area

The southern shelf of the Sea of Marmara covers a broader area (4,194 km^2) compared to the northern one and its average width is 20 km (Gazioğlu et al. 2002; Fig. 3a). The sub-basins in the Bandırma Bay (−51 m) and in the Gemlik Bay (−110 m) are the most distinct geomorphic basins (Fig. 3b). Along the 290-km long southern coasts, the study area covers three sub-basins, namely Erdek, Bandırma and Gemlik, lined up between the Karabiga Promontory in the west and Gemlik Village in the east.

The steep and uplifted shores observed between the Kapıdağ Peninsula (+803 m) and Armutlu Peninsula (+903 m) are mostly fault-controlled. The uplifted region of Karadağ-Bandırma (+750 m), Mudanya (+550 m) and Kurşunlu High-Gemiç Mountains (+520 m at the coast and +1,278 m towards Lake Iznik) forms the most clearly outlined heights along the southern margin of the study area (Fig. 3b). The southern mountains are parallel to the coast and occur in front of the low-lying plains (<100 m) draining the rivers of Kocasu, Gönen and Biga into the Sea of Marmara.

The sedimentary sequence on land ranges from Miocene to recent. The pre-Miocene basement is made up of Cretaceous metamorphic rocks and Paleogene sedimentary units. The basement is distributed over a broad area along the coastal region; the Marmara Islands, Kapıdağ and Armutlu Peninsulas, Karabiga, Karadağ, Kurşunlu, Mudanya and Gemlik (Fig. 4). The basement rocks were covered with volcanic (Lower–Middle Miocene) and sedimentary units (Upper Miocene—Pliocene) behind the coastal mountains. Holocene alluvial units are dominant along the regional rivers and around the lakes of Manyas, Uluabat and Iznik. In the study area, the sedimentary sequences consist of Lower Miocene to younger deposits, which unconformably overlie the pre-Miocene to Miocene basement cropping out on Marmara Island, Karabiga, Kapıdağ and Armutlu Peninsulas (Fig. 4). The units, discordant to each other, are in agreement with the Neogene formations between the lakes Uluabat and Manyas as described by Ergül et al. (1986). The sedimentary units over the folded Miocene basement indicate variable character (Fig. 4) (Marathon Petroleum Turkey 1976). Using single-channel air-gun and deep-tow boomer profiles, Aksu et al. (1999) defined acoustically reflective, lenticular, stratified and cross-stratified deposits (Unit 2) rest on an angular unconformity of sub-unconformity sediments (Unit 3). It is overlain by widespread draping, locally onlapping and acoustically transparent deposits of Unit 1.

Materials and methods

New high-resolution Chirp seismic data (Fig. 3c) were collected in 2010 (350 km of track lines) and 2011 (650 km) using a Bathy 2010P^{TM} Chirp sub-bottom profiler and bathymetric echo sounder which provides high performance sub-bottom survey capability usually for shallow inland waterways by providing algorithms for peak signal detection. The system uses 4 transducers in array configurations to provide full power capability. The power level, sweep bandwidth and detection threshold was adjusted automatically during the survey. The travel times were converted to depth values below the present mean sea level using the typical interval velocities of 1,500 and 1,700 m/s, which have been found to be appropriate for the water column and near-surface siliciclastic sediments (Eriş et al. 2007), respectively. The transmit pulse repetition rate was 1 Hz dependent on the depth range (150 m) and also on the selected pulse length which is short enough to resolve thin layers covering the sub-bottom strata. The penetration depths ranged from a few meters in coarse sand near shore to about 60 m in finer-grained sediments. The vertical resolution of 2–8 kHz source Chirp systems used in this study equates to a theoretical vertical resolution of 0.125 m (assuming a compressional wave velocity of 1,500 m/s). The speed of the research boat was set to 7.0–7.5 km/h during the survey. The ship's position and heading provided with a Magellan Proflex 500 scientific GPS were stored in data files. Following some basic data processing sequences such as gain recovery and filtering using Kogeo Seismic Toolkit 2.7, the seismic sections were interpreted with the aid of seismic-reflection interpretation software Kingdom Suite donated by Seismic Micro Technology.

For a better interpretation, our seismic data were combined with 3 different previous data sets (Fig. 3c) gathered by two other seismic systems with different penetration and resolution characteristics. The first interpreted data set was the single-channel pinger (uniboom) data gathered by the Department of Navigation, Hydrography and Oceanography of Turkish Navy (SHOD) in 1979 (280 km) and 2,000 (150 km) (Tur and Ecevitoğlu 2000; Vardar 2006). Another data set we re-interpreted was the air-gun single-channel analog data collected under the Marmara Gateaway project in 1995 (Aksu et al. 1999, 2000; Yaltırak 2002). All of the seismic data obtained from these previous studies were re-interpreted here and all of the sections given in this paper were not published before.

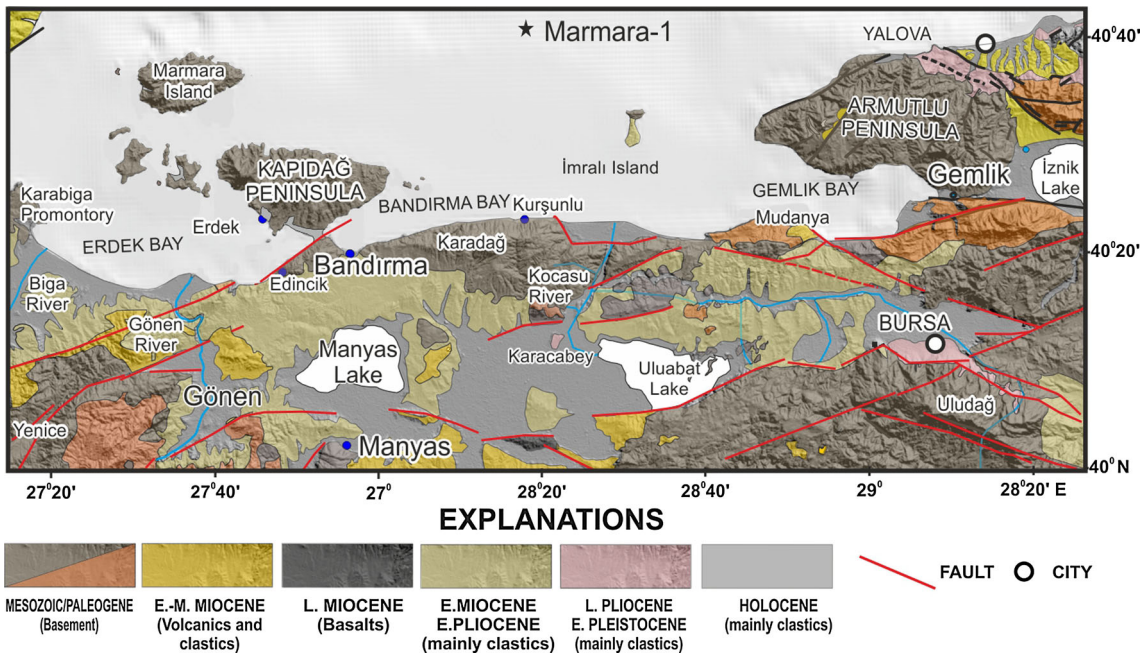

Fig. 4 Simplified geological map of the study area and its surroundings (modified from Yaltırak 2002). The most detailed geological data representing offshore sedimentary units can be obtained from the Marmara-1 borehole, near the shelf edge northwest of the Imralı Island (Marathon Petroleum Turkey 1976)

Multi-beam bathymetric data were collected between 2004 and 2007 during the course of numerous cruises onboard the TCG Çubuklu operated by SHOD (Gökaşan et al. 2010). The system used (Elac-Nautik 1050 D multi-beam sonar) operates with 56 beams at 50 kHz and employs a fan of echo-sounders covering an angle of approximately 120° below the survey vessel. A Sercel NR-203 D-GPS was used for positioning, the vessel speed being held at 15–18 km/h. The corrected data against the ship movements were combined with previous bathymetric maps for the insonified regions by multi-beam sonar and also with topographic elevations digitized from 1:25,000 topographic maps. The combined data were then arranged in 1-m contour intervals using ArcGIS 10 software. For a hillshade presentation using ENVI software program the data were also transformed into a digital elevation model (DEM) as raster files with 30 × 30 m pixel size.

Results

In the present study, three seismic units were distinguished from the high-resolution Chirp seismic reflection profiles from Erdek Bay (Fig. 5a) and from the region between Bandırma and Gemlik Bay (Fig. 5b). These units were named C3, C2 and C1 starting from the sea bottom.

Unit C3: The uppermost seismic unit consists of weak and internally parallel reflectors with coastal onlaps onto Unit C2 (Fig. 5a, b). Unit C3 can be seen everywhere and represents the sedimentation starting from the first marine invasion. It has variable thickness depending on the riverine inputs and geomorphic condition of depositional environments; i.e., it is more than 25 m thick on the Kocasu River delta (Fig. 6a), 19 m in the Gemlik Basin in Gemlik Bay and 12 m in Bandırma Bay. The unit becomes thinner (<2 m) outwards of the Bandırma sub-basin where the acoustic basement uplifted depending on the SEE extension of an underwater ridge forming the small islands to the east of Kapıdağ Peninsula. In Erdek Bay the maximum thickness can be reached in front of the Gönen River as well as at the SE part of the basin; slightly more than 19 and 13 m, respectively (Fig. 6a). Similarly the unit becomes thinner outwards of Erdek Bay, ∼4 m between Karabiga Peninsula and Paşalimanı Island. Unit C3 has variable thickness between the Kapıdağ Peninsula and Marmara Island depending on the sea-bottom morphology (Fig. 6a). Hiscott and Aksu (2002) dated the base of Unit C3 as 9,900 year BP (see Fig 5c and their Figs. 7, 8). On the basis of 15–50 cm thick sapropelic layer at depths ranging from 0.90 to 2.35 m below sea floor, the topmost part of Unit C3 was deposited between about 4,750 and 3,500 ^{14}C year BP during a high global sea-level stand (Çağatay et al. 1999).

Unit C2: This unit is characterized by discontinuous, parallel to sub-parallel, undulating reflections (Fig. 5a, b;7a, b, c). At some localities the unit includes some prograding clinoforms; e.g. offshore Kocasu River (Fig. 7d).

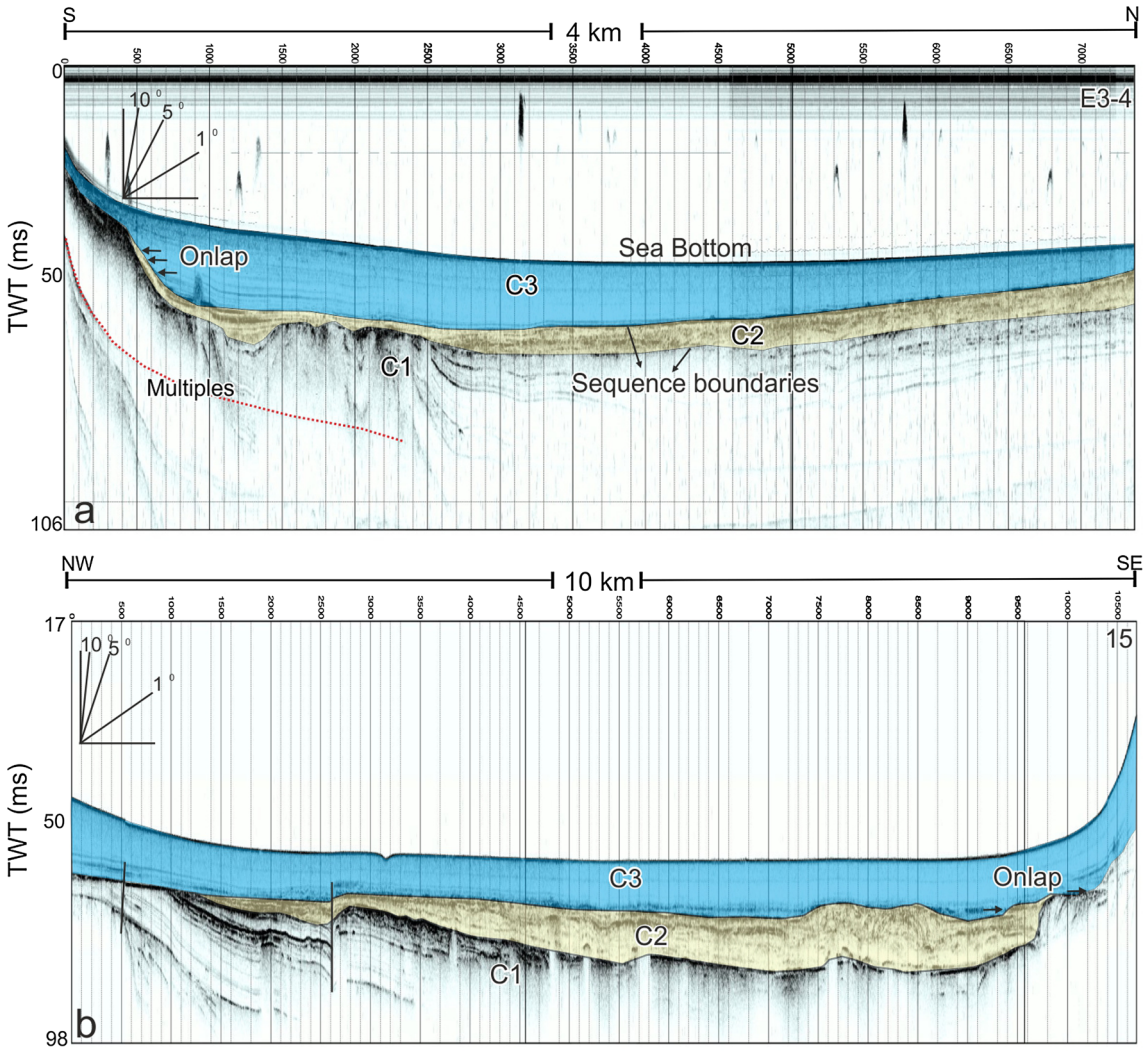

SERIES	CHRONOLOGY		Aksu et al. 1999	Yaltırak and Alpar 2002	Hiscott and Aksu 2002	Kuşçu et al. 2009	This Study
	STAGES	ENVIRONMENT	UNIT	UNIT	UNIT	UNIT	UNIT
QUATERNARY	HOLOCENE	*Marine*	Unit 1	Unit 3 D1	SU A1	Unit 3	C3
				9.7 Kyr	9.9 Kyr		11.3- 11.0 Kyr
		Lacusturine Fluvial	Unit 2	Unit 3 D2	SU A2	Unit 2	C2
				29 Kyr	23 Kyr		30 Kyr
	PLEISTOCENE	*Acoustical Basement*	Unit 3	Unit 2b	B	Unit 1	C1
							(Not to scale)

c

Fig. 5 Interpreted Chirp seismic profiles illustrating the seismic stratigraphic units C1, C2 and C3 **a** line E3-4 in Erdek Bay, **b** line 15 in the Bandırma Bay (see Fig. 3c for locations), **c** seismic units compared with other studies

Unit C2 unconformably overlies a deformed acoustic basement (see Unit C1). The base of Unit C2 forms a major shelf-crossing unconformity surface developed during the last glacial period. The topography of the sequence boundary between Units C3 and C2 becomes deeper, as much as 95 m, from the Kapıdağ Peninsula towards Gemlik Bay (Fig. 6b), implying that the subsidence in the bay was much faster than that in Bandırma Bay. The same sequence boundary in Erdek Bay, on the western side, becomes shallower with a gentle slope towards the northwest (Fig. 6b). Although the average thickness of Unit C2 ranges from 6 to 10 m, it disappears outside the Bandırma Basin

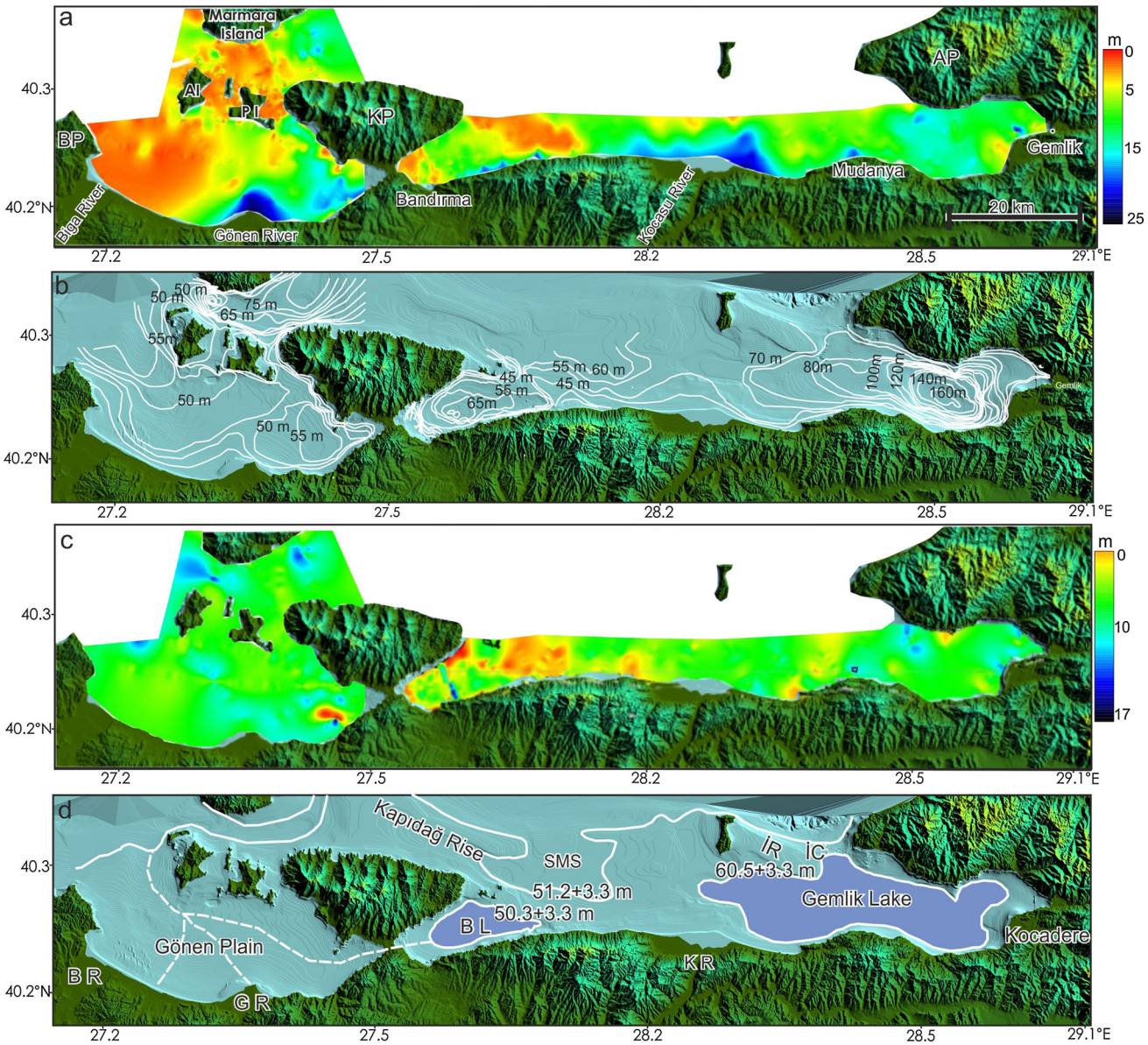

Fig. 6 **a** Isopach map showing sediment thicknesses of Unit C3. *PI* Paşalimanı Island, *AI* Avşa Island, *KP* Kapıdağ Peninsula, *BP* Biga Peninsula *AP* Armutlu Peninsula, **b** depth to the sequence boundary between Units C3 and C2, **c** isopach map showing sediment thicknesses of Unit C2 **d** paleoshoreline of the study area representing the time period of 30,000–11,300–11,000 year BP. *BR* Biga River, *GR* Gemlik River, *KR* Kocasu River, *BL* Bandırma Lake, *SMS* South Marmara Sill, *IR* Imralı Ridge, *IC* Imralı Canyon

(Fig. 6c). Unit C2 was dated to 23,000 year BP by Hiscott and Aksu (2002) (Fig. 5c). On the basis of spatial and temporal distributions of terrestrial and freshwater taxa Mudie et al. (2002) indicated that freshwater conditions were dominant along the southern Sea of Marmara region at 10,800 BP. McHugh et al. (2008) defined that the age of lacustrine sediments to the south of the relatively active Imrali Basin (Fig. 3a) were ~11,800 year BP.

The paleoshoreline between the Imrali Basin and the western end of Armutlu Peninsula was −90 m (Fig. 8a) which becomes shallower westward up to −82.5 m possibly due to relative tectonic uplift (Fig. 8b, c). This represents that the maximum water level of the Marmara paleo-lake was −82.5 m below the present mean sea level. The ocean basins are getting slightly larger since the end of the last glacial cycle because of post-glacial rebound, also called glacial isostatic adjustment (GIA). Therefore the elevations of seismic units and paleoshorelines may be adjusted for GIA which is −0.3 mm/year for this region (Toscano et al. 2011). In that case the paleoshoreline between the Imrali Basin and the western end of Armutlu Peninsula was between −93.5 and −86.0 m with GIA. The Imrali ridge located between the Marmara and Gemlik paleo-lakes caused a water-level

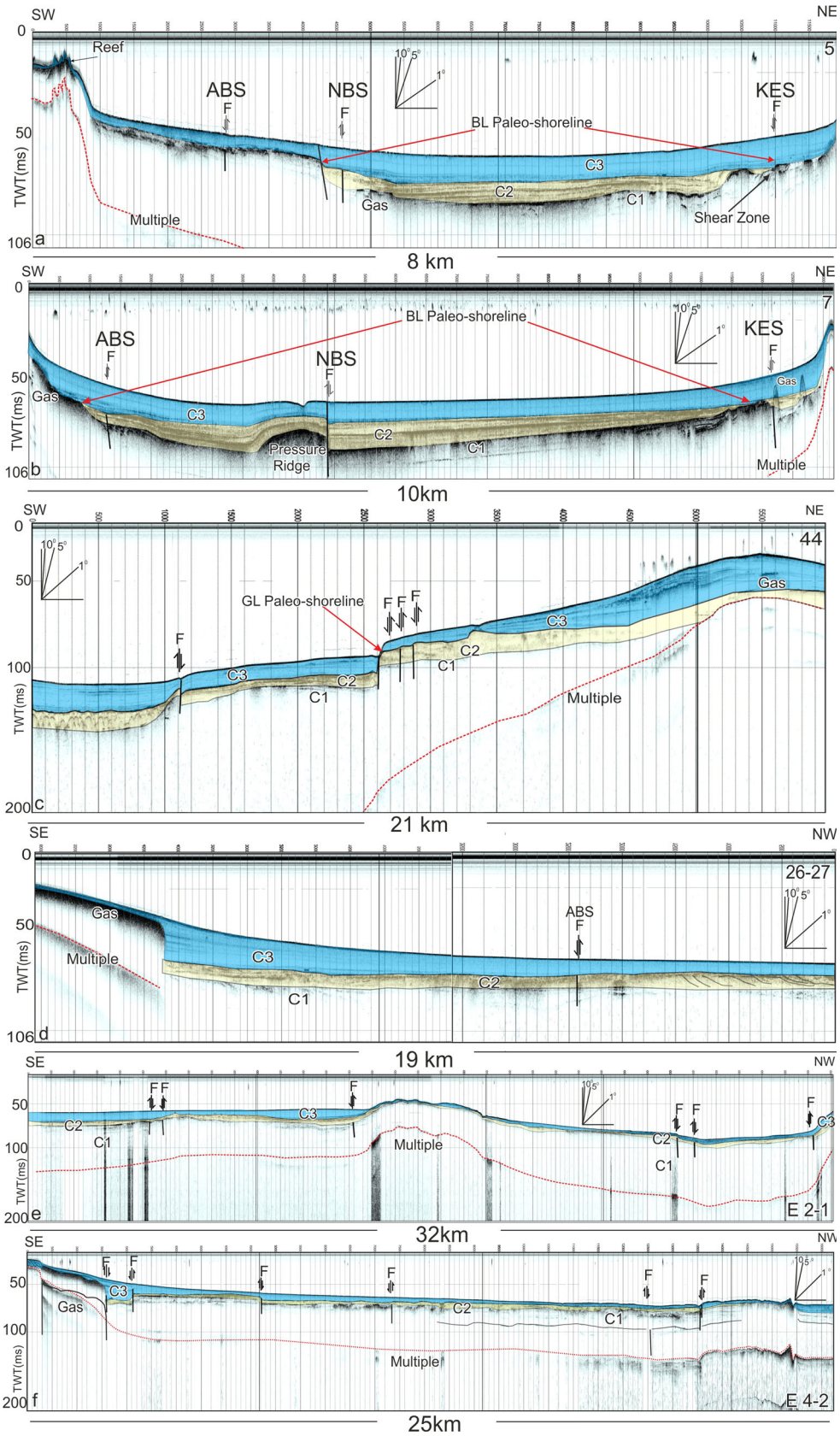

Fig. 7 Interpreted Chirp seismic profiles illustrating **a** the paleoshoreline and NAFMS segments in Bandırma Bay, **b** the pressure ridge, NAFMS segments and paleoshoreline in Bandırma Bay **c** paleoshoreline in Gemlik Bay, **d** the Armutlu Bandırma segment in front of the Kocasu River **e** E–W trending fault south of Marmara Island **f** northwest trending normal faults in Erdek Bay. See Fig. 3c for locations. *ABS* Armutlu Bandırma segment, *NBS* new Bandırma segment, *KES* Kapıdağ Edincik segment, *BL* Bandırma Lake, *GL* Gemlik Lake

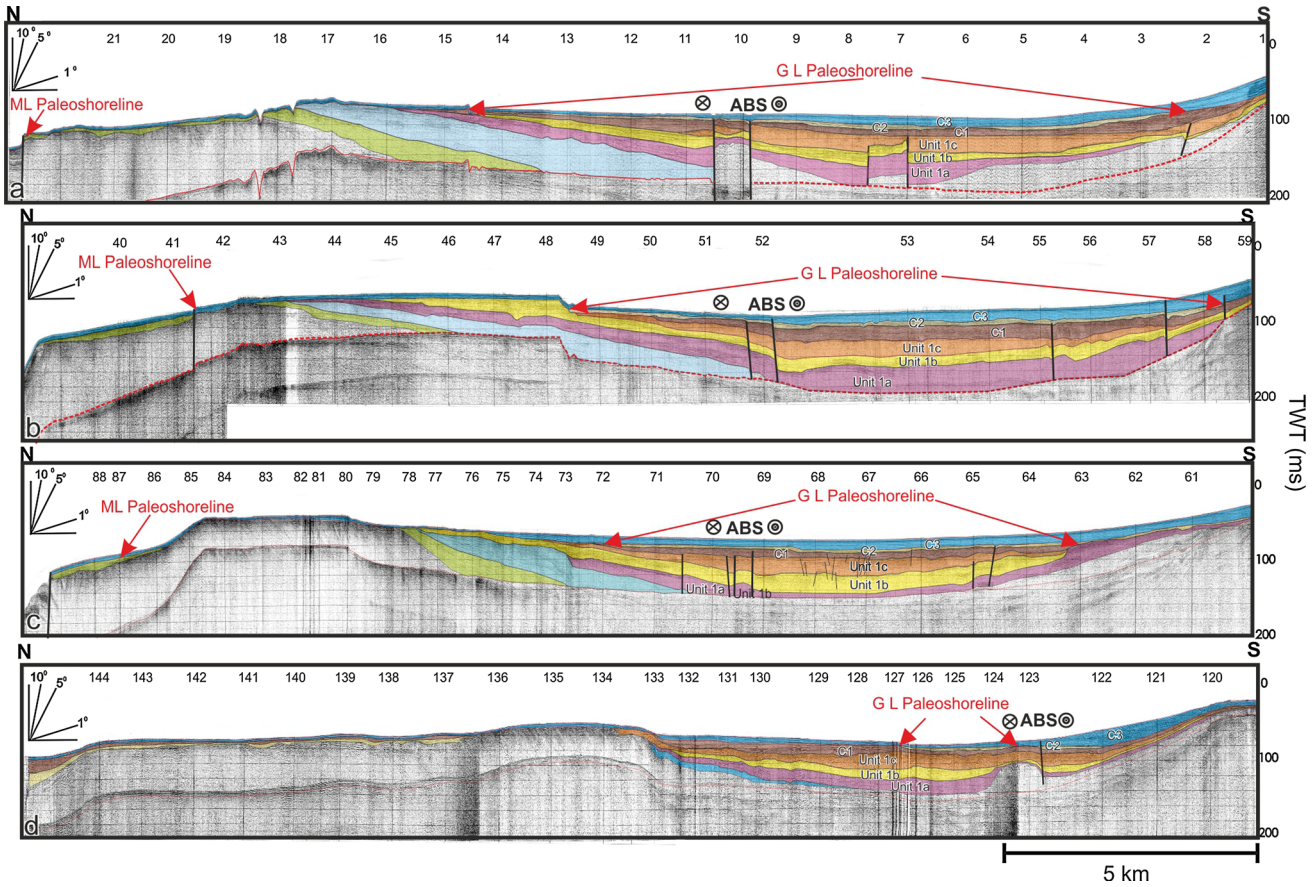

Fig. 8 Interpreted seismic pinger (uniboom) profiles, oriented north–south, illustrating the Armutlu-Bandırma segment (ABS) and the paleoshorelines of the paleolake Gemlik (GL) and paleolake Marmara (ML) **a** line 1–23, **b** line 39–59, **c** line 61–90, **d** line 120–145. See Fig. 3c for locations

difference of 23 m (at least) between these two aquatic environments.

Unit C1: This is the deepest sedimentary package constituting the folded basement in the Chirp data. The interface between Units C1 and C2 represents the upper surface of the Early–Middle Pleistocene sediments identified in the sea (Fig. 5a, b). Its internal stratification varies throughout the study area from parallel divergent to undulating reflections depending on the topography. Unit C1 represents the deposits on the shelf formed during a period of relatively faster sea level rise. This unit corresponds to Unit 1 defined by Kuşçu et al. (2009) and Unit 2b defined by Yaltırak and Alpar (2002a) (Fig. 5c), which is older than 30,000 year.

Paleoshoreline

The Sea of Marmara is a transcontinental water passage between the Mediterranean and Black Seas. The water exchange between these two seas is controlled by two respective sills. The first is located in the Strait of Istanbul (Bosphorus) and the other is offshore Şarköy to the east of the Strait of Çanakkale (Dardanelles). Their depths are −35 and −70 m, respectively. These sills prevented a seawater connection between Black Sea and Mediterranean Sea during the later Quaternary (Stanley and Blanpied 1980) while the sill in the Dardanelles also controlled the water level of the Sea of Marmara during global lowstands (Smith et al. 1995). Thus the water-level fluctuations of the Sea of Marmara, limited in magnitude by the sill depth of the Strait of Dardanelles, are small in amplitude (e.g., 70 m) but enough to change its condition into a lacustrine paleoenvironment (Aksu et al. 1999; Yaltirak 2002; Çağatay et al. 2002; Aksu et al. 2002; Kaminski et al. 2002). If we consider that the elevation of a paleoshoreline has not changed since deposition, then the measured elevation is equal to the sea level at that geological period. So the evolution time of the paleoshoreline outlined from our seismic data was defined regarding the bathymetric relation between the sub-basins and the Sea of Marmara, as well as considering the global sea-level curve given by Bard et al. (1990, 1996, 2010) and Stanford et al. (2011).

The paleo-lake shoreline was identified depending on the termination of lake deposits (Unit C2) on the coastal region and the terrace-shaped geometry of the upper surface of Unit

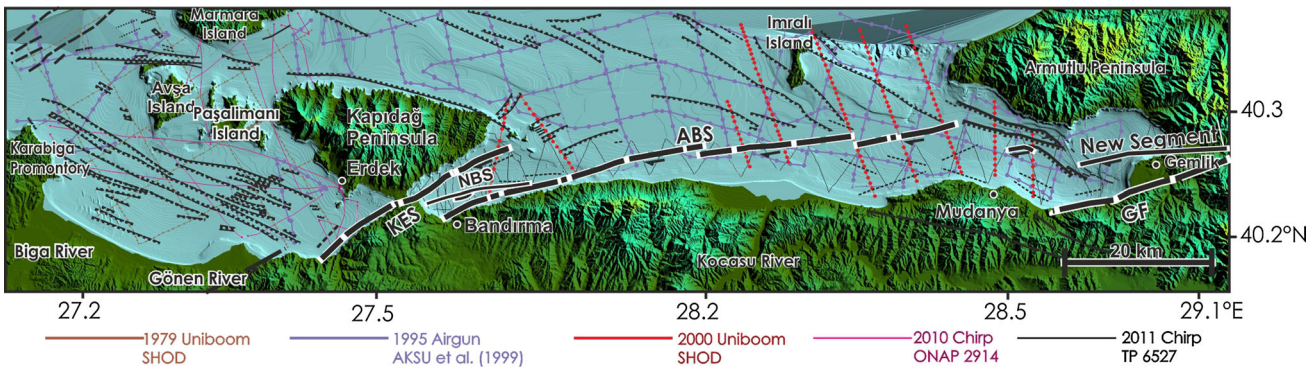

Fig. 9 The structural model proposed for the study area on the basis of seismic reflection and multibeam bathymetric data. *GF* Gençali fault, *ABS* Armutlu-Bandırma segment, *KES* Kapıdağ-Edincik segment, *NBS* new Bandırma segment

C2. This surface becomes shallower westward, from Gemlik Bay to Bandırma Bay (Fig. 6b). In Erdek Bay it gets shallower northwestward gradually with a slight slope (Fig. 6b). The paleoshoreline could also be identified on the multibeam data if it is integrated with some normal faults trending along the shoreline; e.g. at the eastern part of Gemlik Bay (Fig. 7c). Since the paleoshorelines correspond to 11,000–11,300 year BP when the sea level overtopped the southern Marmara sill, the total GIA correction was approximately 3.3 m for the paleoshorelines. Considering GIA these shorelines, in other words the highest terrace levels, were located at −50.3 m (−53.6 m with GIA) in Bandırma Bay (Fig. 7a, b) and −60.5 m (−63.8 m with GIA) in Gemlik Bay (Figs. 7c; 8a–d).

The coastal features of a paleolake were outlined on the seismic sections and occupied the basin in Gemlik Bay and extended into the front of the Kocasu River mouth (Fig. 6d). The paleolake was receiving drainage and fed by the paleo-rivers in the region. To the east of Imralı Island a long and relatively narrow underwater valley at −60 m (−63.5 m with GIA) water depth is the most outstanding sea-bottom feature on the multibeam bathymetric map (Fig. 3b). This canyon's role can be explained by the existence of this paleolake, as it must carry the lake waters into the deeper basins of the Sea of Marmara and control the level of the paleolake. The seismic data show another isolated paleolake located in the vicinity of Bandırma Bay (Fig. 6d). It was possibly discharging westward into Erdek Bay through a water passage between the Kapıdağ Peninsula and its mainland, which was closed by Belkis Isthmus at least 2,500 years BP (Ardel and Inandik 1957). On the multibeam bathymetry, some small-scale seafloor mounds observed at the easternmost part of Erdek Bay (Fig. 6d) may be dependent on an outward flow coming from the Bandırma paleolake. The development of Belkis Isthmus, which is placed on top of the highest part of an autochthonous ridge lying between the Bandırma and Erdek depression fields, is not well known. It is made up of two opposite coastal spits, which are developed seaward from the shores into the sea utilizing suitable promontories of the autochthonous ridge, and then separated the bays of Bandırma and Erdek. The swamp area in the central part was a remnant of a lagoon (Ardel and Inandik 1957).

Structural setting and new fault segment

The NAFMS is made up of three segments between Bandırma and Gemlik Bays (Fig. 9). The easternmost segment is on land and is known as the Gençali fault between the southern coast of Lake Iznik and Mudanya. A west-trending active fault cuts the uppermost seismic unit C3 at the eastern part of Gemlik Bay and extends towards the deep basin of Gemlik Bay, in front of the northern part of the Gençali delta and parallel to the coastline (Fig. 9). This active fault was interpreted as a "new segment". At present the Gençali fault is no longer active and its slip has been transferred to the new segment.

The second segment is an active fault, 75 km long from the northern margin of Gemlik Bay to the southern part of Bandırma Bay (Figs. 7a, b, d;8a–d). This segment, called the Armutlu-Bandırma segment (ABS), is made up of three sub-segments separated by small offsets. Such step-overs are common features on long strike-slip fault systems.

In Bandırma Bay, the NAFMS makes a big offset toward the southeastern shores of the Kapıdağ Peninsula and is connected to the Edincik Fault along the southern flank of the Erdek Bay trough (Fig. 9). It is called the Kapıdağ-Edincik segment (KES) (Fig. 7a, b). The angle between the KES (N59E) and the ABS at the south of Bandırma Bay (N75E), which is 16° (Fig. 9), caused a pressure ridge in the central part of Bandırma Bay (Fig. 7b). Another N85E trending fault, the New Bandırma Segment (NBS), is active and cut through the deepest part of Bandırma Bay (Figs. 7a, b, 9).

Even though there are some secondary faults of the NAFMS affecting the sediments at the southeastern margin of Erdek Bay, most of the structural elements in this westernmost basin are northwest-southeast trending normal faults (Fig. 9) and are not deforming the seismic units defined in this study (Fig. 7e, f). Another strike-slip fault system (Fig. 7e), however, crosses and affects the sediments to the south of Marmara Island (Fig. 9).

Discussion

Unit C2 was deposited on the acoustic basement (Unit C1) between 30,000 and 11,000–11,300 year BP, when the sea level was below the southern Marmara sill (−51.2 m without −3.3 m GIA). Parallel to subparallel, occasionally sigmoid and oblique reflections of Unit C2 represent riverine and lacustrine depositional environments. Its deposition depends on the water depth and sea floor morphology. Unit C2 was mentioned with different nomenclature in previous studies (Fig. 5c); Unit 2 accreting sand bars by Aksu et al. (1999), Unit 3-D2 by Yaltırak and Alpar (2002a) and Unit 2 by Kuşçu et al. (2009). Considering the depth of the Şarköy sill (−70 m) and the sea-level records given by Stanford et al. (2011), the post glacial connection of the Sea of Marmara with the Aegean Sea occurred between 12,350 and 12,800 year BP (Fig. 10). The paleoshorelines of the early Holocene lake in the Gemlik basin (−60.5 m below present mean sea level without GIA) and the Marmara lake margin (which changed between −83 and −90 m below present mean sea level, without GIA) at the Imrali Basin (Fig. 8a–c) are directly related to this event. Unit C3 started to be deposited on the southern Marmara shelf after sea level

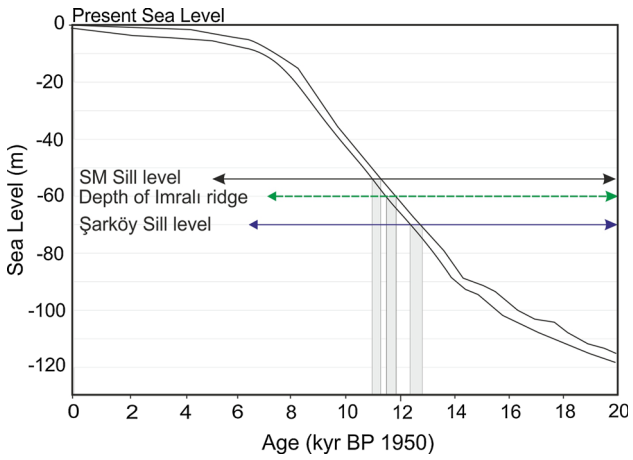

Fig. 10 The elevation of the ridges controlling water connections in the Sea of Marmara depicted on the glacio-eustatic sea level changes for the last 20,000 year BP given by Stanford et al. (2011). See Fig. 1 for Şarköy sill level and Fig. 3b for southern Marmara sill and Imralı ridge

overtopped the southern Marmara sill (Fig. 6d). In the previous studies this unit was also called a transparent Unit 1 mud drape (Aksu et al. 1999), Unit 3-D1 (Yaltırak and Alpar 2002a) and Unit 3 (Kuşçu et al. 2009; Fig. 5c).

Two large paleolakes in Gemlik and Bandırma Bays can be traced from the paleoshorelines at −60.5 m without −3.3 m GIA (Figs 7c, 8a–d), −50.3 m without −3.3 m GIA (Fig. 7a, b) and from the multibeam bathymetry where the shorelines are fault controlled (Fig. 6d). This setting is similar to the present topographic conditions observed between the Sea of Marmara and the shallow freshwater lakes in the southern Marmara region, which are depositional areas on the courses of main rivers. With an elevation of 15 m above the present mean sea level, Lake Manyas reaches a depth of 3 m. On the other hand, the water level of Lake Uluabat is +1 m above sea level, since it is connected to the Sea of Marmara by the Kocasu River (Fig. 4).

The boundaries of the paleolake we defined in Gemlik Bay are somewhat different than those given by Yaltirak and Alpar (2002a, their Fig. 11J). The Gemlik paleolake was fed by the surrounding rivers and discharged into the Imralı Basin located to the east of Imralı Island (Fig. 6d), similar to the Kocasu River connecting the Lake Uluabat to the Sea of Marmara today (Fig. 4).

The paleolake in Bandırma Bay, on the other hand, was not controlled by rivers. It was discharging into Erdek Bay via a paleo-channel located at the southern margin of the Kapıdağ Peninsula before the modern isthmus was developed (Fig. 6d). The lack of any erosional truncation surface related to a paleoshoreline in Erdek Bay and the paleo-river observed on the multibeam data indicate that a riverine regime was dominant in the region with poorly drained marsh areas and plains during early phase of sea level rise (Fig. 6d).

Contrary to a single fault segment as proposed by Kurtuluş and Canbay (2007), the NAFMS is a right-lateral strike-slip fault that is made up of three main segments in the sea with step-overs (Fig. 9). The Armutlu-Bandırma segment cuts through the seismic units C1 and C2 (Figs. 7a, b, d, 8) and partly affects the uppermost marine sediments (Unit C3) younger than 11,000–11,300 year BP (Fig. 8a, b, d). As far as it is known no big earthquakes have occurred on this segment for the last few thousand years (e.g., Guidoboni 1994; Ambrasseys 2009).

The northwest–southeast faults in Gemlik Bay have evolved over the Thrace-Eskisehir Fault system (Fig. 1). They were cut through by the NAFMS, giving way to the formation of extensional step-over geometry. Under the new tectonic regime, Gemlik Bay opened as a pull-apart basin between the Gençali fault and Armutlu-Bandırma segment (Fig. 9), similar to the 30° extensional sidestep model given by Dooley and McClay (1997). This is in agreement with the models proposed by Barka and Kuşçu (1996), Yaltırak and

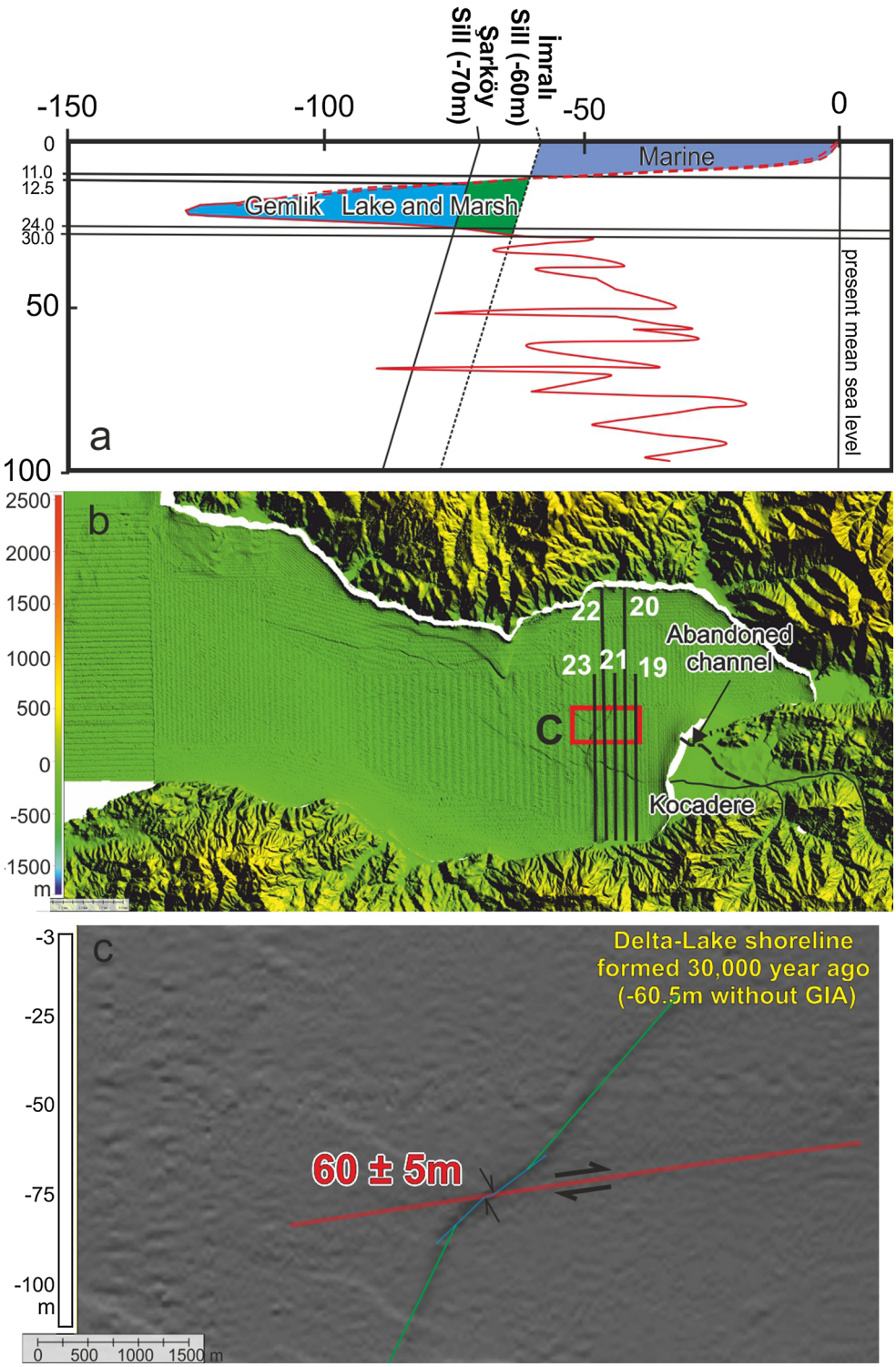

Fig. 11 **a** Sequence stratigraphic interpretation of observed stratigraphic architecture and proposed chronostratigraphic framework, based on correlation of seismic units in Gemlik Bay with late quaternary glacio-eustatic sea level changes. Sea level curve after Chappell and Shackleton (1986) and Bard et al. (1990), recent 20,000 year is from Stanford et al. (2011) **b** seismic lines given in Fig. 12 (Kuşçu et al. 2009) superimposed on the multibeam bathymetry, **c** the total displacement occurred on the shoreline of the progressive delta during the last 30,000 years on the multibeam bathymetry map

Alpar (2002a) and Gasperini et al. (2011). The pull-apart system, which started to evolve with the Gençali fault, transformed into a new regime (NS) parallel to the evolution of the paleolake of Gemlik at 30,000 BP when the sea level was −60.5 (−3.3 m GIA) (Fig. 11a) and the NAFMS took over a new fault between Lake Iznik and Gemlik Bay (Fig. 9). The mouth of the main stream which formed the Gençali delta at that time was located somewhere to the north of the actual Kocadere stream delta at the eastern edge of the bay (Fig. 11b). The delta front, which was forming the eastern coastline of the paleolake, was cut through by the W-trending new segment (Fig. 9). A right-lateral narrow

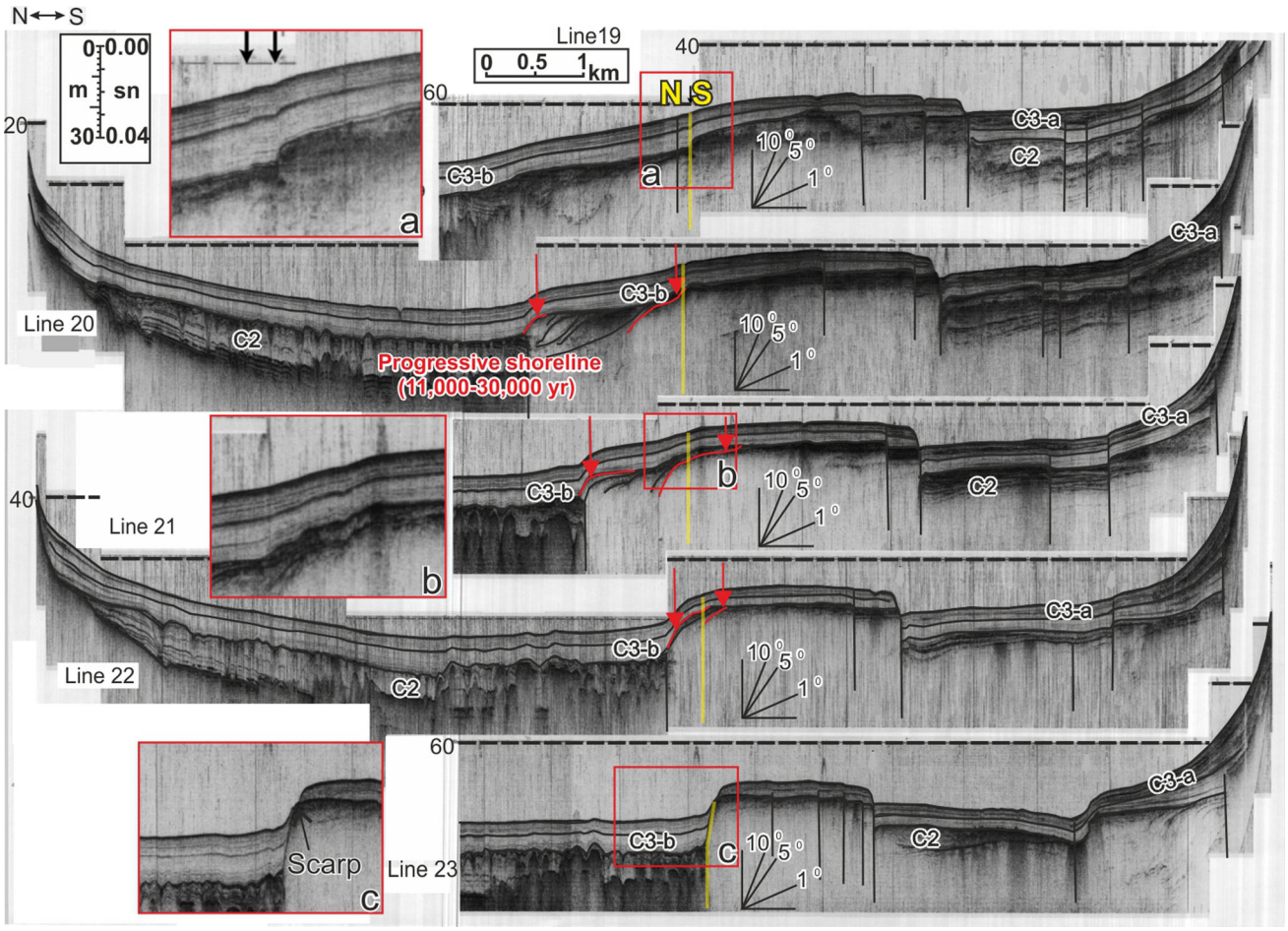

Fig. 12 Re-interpreted shallow Chirp seismic profiles published by Kuşçu et al. (2009). The data are recorded on the topographic high of the lacustrine delta drowned after the last episode of sea level rise and given in Fig. 11b. *Yellow lines* show the new segment developed on the NAFMS while the *red arrows* show the prograding foresets of the lower and upper chronostratigraphic boundaries. *NS* new segment

and rectilinear slip of the paleoshoreline can be seen on the morphobathymetric data, with an offset of 60 ± 5 m (Fig. 11c). Considering the evolution of the Gemlik paleolake of during the last 30,000 year BP, the lateral slip rate on the NAFMS corresponds to 2 mm/year, which is consistent with geodetic models given by Straub et al. (1997), McClusky et al. (2000), Meade et al. (2002) and Ergintav et al. (2007).

Using the same lacustrine delta displacement on a lobate topographic high, Gasperini et al. (2011) estimated the horizontal slip rate for the NAFMS on the order of 4 mm/year. The researchers suggested that the delta front was inactive and passively displaced by the NAFMS when marine conditions started 11,000 year BP. However, there was no sea connection between the Gemlik and Marmara paleolakes when the sea level was below −60.5 m. Therefore the coastline of the isolated paleolake stayed approximately at −60.5 m (with a slight decrease and subsequent increase) when global sea level was below the Imrali canyon's depth. In that case the deltaic sequence above −60.5 m in the seismic sections was started at 30,000 BP and ended (drowned) at 11,300–11,000 year BP. This can be supported by the lacustrine delta front representing a descending trajectory progressive morphobathymetric shoreline as observed on sections 20, 21 and 22 in Fig. 12. During the development of the progressive shoreline of the Gemlik paleolake, the upper parts of the progressive deltas were eroded at some localities and a natural scarp was formed in front of the delta lobe to the west (Line 23 in Fig. 12). The age of the erosion surface of the natural scarp, where we calculate the total offset on multibeam bathymetry, is 30,000 year. Therefore we suggest the horizontal slip rate for the NAFMS was on the order of 2 mm/year. In addition, the core Marm05–124 of Gasperini et al. (2011) is close to the mouth of the modern Kocadere stream, which cannot represent such a displacement (Fig. 11b). Naturally the core locality represents only a coastal plain at 11,000 year BP which was later drowned by the rising sea-level in the Sea of Marmara. Therefore the estimated slip rates given by Gasperini et al. (2011) and their calculation for the amount of stress accommodated along the NAFMS are not consistent

sufficiently either with the available geodetic models (Straub et al. 1997; McClusky et al. 2000; Meade et al. 2002; Ergintav et al. 2007) or with other interpretations on total displacement (Yaltırak 2002; Yaltırak and Alpar 2002a).

Bandırma Bay is interpreted as a rectangular transpressional basin developed under the control of the 16° angle difference between the segments of Kapıdağ-Edincik and Armutlu-Bandırma, which are bordering the shorelines of the Kapıdağ Peninsula and the southern coastline of the bay, respectively (Fig. 9). Considering the faults affecting the younger deposits and bordering the pressure ridge (Fig. 7b), a younger W-trending fault (NBS) was mapped between the oblique segments of Kapıdağ-Edincik and Armutlu-Bandırma (Fig. 9). In large scale similar morphological elements to those in the Bandırma Bay can be seen in the western Marmara trough (Yaltırak 2002; Yaltırak and Alpar 2002b). The difference between these basins in their size and depths can be explained by the faster lateral movement of the NAFNS (19 mm/year) according to that of NAFMS (2 mm/year). Meanwhile the transpressional deformations experienced by strike-slip shear and component shortening due to southwestward bending of the faults, in concordance with the horizontal velocity field (see GPS vectors in Fig. 3a; Ergintav et al. 2007), resulted in oblique shear in both basins. If Bandırma Bay had been deepened as a transtensional basin due to step-over geometry, then the deepest part of the basin and the thickest deposits would have been at the NE margin of the basin and in front of a NW–SE oriented normal fault. In contrary the deepest sea bottom and the thickest deposits are located at the western margin, where Bandırma Bay becomes narrow. Therefore the development of the Bandırma Basin depends on the existence of a thrust component in addition to the strike-slip components of the boundary faults.

The NWW–SEE trending normal faults in Erdek Bay have no effect on the seismic units C2 and C3 (Figs. 7e, f, 9). These faults may have developed before the NAF regime when the TEF was active in the region. Moreover, Erdek Bay developed as a passive basin, even though the southeastern margin of Erdek Bay is under the control by the secondary faults of the NAFMS.

Conclusion

The seismic data taken from southern Marmara sub-basins present three seismic units which indicate that the Sea of Marmara experienced fluctuations in sea level. The most characteristic seismic unit is made up of lacustrine-fluvial sediments (Unit C2) overlying unconformably an acoustical basement (C1) and overlain by the internally parallel reflectors of marine deposits (C3). Following the post-glacial connection of the Sea of Marmara with the Aegean Sea (12,350–12,800 year), two paleolakes were still in Gemlik and Bandırma Bays, respectively. Considering global isostatic adjustment, which is about 3.3 m for the last 11,000 years, the water levels in these lakes were limited by the sill depth of the Southern Marmara Sill, and can be rounded to −55 m. This sill controlled the marine incursion of these sub-basins by the Sea of Marmara until ~11,300–11,000 years BP depending on the modelled sea-level probabilities given by Stanford et al. (2011). Before the marine incursion the shorelines of the Gemlik and Bandırma paleolakes were located approximately −64 and −54 m below the present sea level, respectively. The Gemlik paleolake was discharging into the Imralı basin via the Imralı canyon which was approximately -63 m bmsl.

Gemlik Bay opened between the Armutlu-Bandırma fault segment and the Gençali Fault as a pull-apart basin. The northwest-southeast trending fault systems, which are bounding the bay and extending into the Sea of Marmara, were developed on the remnants of the Thrace-Eskisehir Fault. This active pull-apart system was cut through with a new W-trending fault segment extended from the Lake Iznik into Gemlik Bay for at least the last 30,000 years. Its right-lateral offset on the lacustrine delta drowned after the last episode of sea level rise is 60 ± 5 m, which corresponds to a slip rate of 2 mm per year.

The Armutlu-Bandırma segment of the NAFMS, which is 75 km long from the northern margin of Gemlik Bay to the southern part of Bandırma Bay, is made up of three subsegments separated by short oversteps. The western subsegment of Armutlu-Bandırma is divergent to the Kapıdağ-Edincik segment forming a rectangular transpressional basin. A new west-east trending fault (NBS) cuts this system causing a pressure ridge at the southern margin of Bandırma Bay. Finally, Erdek Bay in the west is a passive basin under the control of northwest-southeast trending faults.

Acknowledgments This study was supported by the Scientific Research Fund of Istanbul University under the projects of ÖNAP-2914 for Chirp data acquisition in Erdek Bay and around the Marmara Islands, TP-6527 for seismic profiling between Bandırma and Gemlik Bays and UDP-36083 for a travel grant. We thank the officers and crew, as well as the scientists and technicians onboard the TCG Çubuklu and TCG Çeşme of the Turkish Navy, Department of Navigation, Hydrography, and Oceanography, for multibeam and seismic data. The authors thank to Dr. Ali Aksu for seismic lines from Marmara Sea Gateaway project and research assistant Irem Elitez for her drawings of topographic and bathymetric maps.

References

Adatepe F, Demirel S, Alpar B (2002) Tectonic setting of the southern Marmara Sea region: based on seismic reflection data and gravity modeling. Mar Geol 190:383–395

Aksu AE, Hiscott RN, Yaşar D (1999) Oscillating Quaternary water levels of the Marmara Sea and vigorous outflow into the Aegean Sea from the Marmara Sea-Black Sea drainage corridor. Mar Geol 153:275–302

Aksu AE, Calon TJ, Hiscott RN, Yaşar D (2000) Anatomy of the North Anatolian Zone in the Marmara Sea, Western Turkey: extensional basins above the continental transform. GSA Today 10:3–7

Aksu AE, Hiscott RN, Kaminski MA, Mudie PJ, Gillespie H, Abrajano T, Yaşar D (2002) Last glacial–Holocene paleoceanograph of the Black Sea and Marmara Sea: stable isotopic, foraminiferal and coccolith evidence. Mar Geol 190:119–149

Alpar B, Çizmeci S (1999) Seismic hazard assessment in the Gemlik Bay region following the 17 August Kocaeli Earthquake. Turk J Mar Sci 5:149–166

Ambrasseys N (2009) Earthquakes in the eastern Mediterranean and the Middle East: a multidisciplinary study of 2000 years of seismicity. Cambridge University Press, Cambridge. ISBN:978-1-4020-8221-4

Ardel A, Inandık H (1957) Isthmus at Kapidag Peninsula (Belkıs Tombolosu) (in Turkish with English abstract). Coğrafya Enstitüsü Dergisi 8:65–66

Bard E, Hamelin B, Fairbanks RG (1990) U-Th ages obtained by mass spectrometry in corals from Barbados: sea level during the past 130000 years. Nature 346:456–458

Bard E, Hamelin B, Arnold M, Montaggioni L, Cabioch G, Faure G, Rougerie F (1996) Deglacial sea level record from Tahiti corals and the timing of meltwater discharge. Nature 382:241–244

Bard E, Hamelin B, Sabatien DD (2010) Deglacial meltwater pulse 1B and Younger Dryas sea levels revisited with boreholes at Tahiti. Science 327(5970):1235–1237

Barka AA, Kadinsky-Cade K (1988) Strike-slip fault geometry in Turkey and its influence on earthquake activity. Tectonics 7:663–684

Barka AA, Kuşçu I (1996) Extents of the North Anatolian fault in the Izmit, Gemlik and Bandırma Bays. Turk J Mar Sci 2:93–106

Çağatay MN, Algan O, Sakınç M, Eastoe CJ, Balkıs, Egesel N, Ongan D, Caner H (1999) A mid-late Holocene sapropelic sediment unit from the southern Marmara sea shelf and its palaeoceanographic significance. Quat Sci Rev 18:531–540

Çağatay MN, Görür N, Algan O, Eastoe CJ, Tchapalyga A, Ongan D, Kuhn T, Kuşçu I (2002) Late Glacial–Holocene paleoceanography of the Sea of Marmara: timing connections with the Mediterranean and the Black Seas. Mar Geo 167:191–206

Chappell J, Shackleton NJ (1986) Oxygen isotopes and sea level. Nature 324:137–140

Dooley T, McClay KR (1997) Analog modeling of pull-apart basins. AAPG Bull 81:1804–1826

Ergin M, Kazanci N, Varol B, Ileri Ö, Karadenizli L (1997) Sea-level changes and related depositional environments on the southern shelf. Mar Geol 140:391–403

Ergintav S, Doğan U, Gerstenecker C, Çakmak R, Belgen A, Demirel H, Aydın C, Reilinger R (2007) A snapshot (2003–2005) of the 3D postseismic deformation for the 1999, Mw = 7.4 Izmit earthquake in the Marmara Region, Turkey, by first results of joint gravity and GPS monitoring. J Geodyn 44:1–18

Ergül E, Gözler Z, Akçagören F, Öztürk Z (1986) Geology map of Turkey, Bandırma E6 section, scale 1:100000. General Directorate of Mineral Research and Exploration, Ankara

Eriş KK, Ryan WBF, Cagatay MN, Sancar U, Lericolais G, Menot G, Bard E (2007) The timing and evolution of the post-glacial transgression across the Sea of Marmara shelf south of Istanbul. Mar Geo 243:57–76

Gasperini L, Polonia A, Çağatay MN, Bortoluzzi G, Ferrante V (2011) Geological slip rates along the North Anatolian Fault in the Marmara region. Tectonics, 30:TC 6001. doi:10.1029/2011TC002906

Gazioğlu C, Gökaşan E, Algan O, Yücel ZY, Tok B, Doğan E (2002) Morphologic features of the Marmara Sea from Multibeam data. Mar Geol 190:397–420

Gökaşan E, Tur H, Ergin M, Görüm T, Batuk FG, Sağcı N, Ustaömer T, Emem O, Alp H (2010) Late quaternary evolution of the Çanakkale Strait region (Dardanelles, NW Turkey): implications of a major erosional event for the postglacial Mediterranean-Marmara Sea connection). Geo Mar Lett 30:113–131

Gökçeoğlu C, Tunusluoğlu MC, Görüm T, Tur H, Gökaşan E, Tekkeli AB, Batuk F, Alp H (2009) Description of dynamics of the Tuzla landslide and its implications for further landslides in the northern slope and shelf of the Cinarcik Basin (Marmara Sea, Turkey). Eng Geol 106(3–4):133–153

Guidoboni E (1994) Cataloque of Ancient Earthquakes in the Mediterranean area up to the 10th Century instituto Nazionale di Geofisica, Roma. Instituto Nazionale di Geofisica, Rome. ISBN:88-85213-06-5

Gürer ÖF, Kaymakçı N, Çakır Ş, Özburan M (2003) Neotectonics of the southeast Marmara region, NW Anatolia, Turkey. J Asian Earth Sci 21(9):1041–1051

Hiscott RN, Aksu AE (2002) Late Quaternary history of the Marmara Sea and Black Sea from high-resolution seismic and gravity core studies. Mar Geol 190(1–2):261–282

Kaminski MA, Aksu AE, Box M, Hiscott RN, Filipescu S, Al-Salameen M (2002) Late glacial to Holocene benthic foraminifera in the Marmara Sea: implications for Black Sea Mediterranean Sea connections following the last deglaciation. Mar Geol 190:165–202

Kavukçu S (1990) Active fault investigation in Izmit Bay, Bandirma Bay and Erdek Bay of Marmara Sea, historical seismicity and seismotectonics of the Mediterranean Region. In: Proceedings Turkish atomic energy authority, pp 238–266

Koçyiğit A (1988) Tectonic setting of the Geyve basin: age and total displacement of Geyve fault zone. METU Pure Appl Sci 21:81–104

Kurtuluş C, Canbay MM (2007) Tracing the middle strand of the North Anatolian fault zone through the southern Sea of Marmara based on seismic reflection studies. Geo Mar Lett 27:27–40

Kuşçu I, Okamura M, Matsuoka H, Yamamori K, Awata Y, Özalp S (2009) Recognition of active faults and stepover geometry in Gemlik Bay, Sea of Marmara, NW Turkey. Mar Geol 260:90–101

Marathon Petroleum Turkey (1976) Marmara–1. Final well report, p 26

McClusky S, Balassanian S, Barka A, Demir C, Ergintav S, Georgiev I, Gürkan O, Hamburger M, Hurst K, Kahle H, Kastens K, Kekelidze K, King R, Balassanian S, Barka A (2000) Global positioning system constraints on plate kinematics and dynamics in the eastern Mediterranean and Caucasus. J Geophys Res 105:5695–5719

McHugh CMG, Gurunga D, Giosanc L, Ryan WBF, Mart Y, Sancar U, Burckle L, Çagatay MN (2008) The last reconnection of the Marmara Sea (Turkey) to the World Ocean: a paleoceanographic and paleoclimatic perspective. Mar Geol 255:64–82

Meade BJ, Hager BH, McClusky RE, Reilinger S, Ergintav S, Lenk O, Barka AA, Özener H (2002) Estimates of seismic potential in the Marmara region from block models of secular deformation constrained by global positioning system measurements. Bull Seismol Soc Am 92:208–215

Mudie PJ, Rochon A, Aksu AE (2002) Pollen stratigraphy of late quaternary cores from Marmara Sea: land-sea correlation and paleoclimatic history. Mar Geol 190:233–260

Öztürk K, Yaltırak C, Alpar B (2009) The relationship between the tectonic setting of the Lake Iznik Basin and the Middle Stand of the North Anatolian fault. Turk J Earth Sci 18:209–224

Rangin C, Demirbağ E, Imren C, Crusson A, Normand A, Le Drezen E, Le Bot A (2002) Marine Atlas of the Sea of Marmara, (Turkey). IFREMER, ISBN:2-84433-068-1

Selim HH, Tüysüz O, Karakaş A, Taş KÖ (2013) Morphotectonic evidence from the southern branch of the North Anatolian Fault (NAF) and basins of the south Marmara sub-region, NW Turkey. Quat Int 292:176–192

Şengör AMC (1979) The North Anatolian transform fault; its age offset and tectonic significance. J Geol Soc Lond 136:269–282

Smith AD, Taymaz T, Oktay F, Yüce H, Alpar B, Başaran H, Jackson JA, Kara S, Şimşek M (1995) High resolution seismic profiling in the Sea of Marmara (northwest Turkey): late quaternary sedimentation and sea-level changes. GSA Bull 107:923–936

Stanford JD, Hemingway R, Rohling EJ, Challenor PG, Medina-Elizalde M, Lester AJ (2011) Sea-level probability for the last deglaciation: a statistical analysis of far-field records. Global Planet Change 79(3–4):193–203

Stanley DJ, Blanpied C (1980) Late quaternary water exchange between the eastern Mediterranean and the Black Sea. Nature 266:537–541

Straub C, Kahle HG, Schindler C (1997) GPS and geologic estimates of the tectonic activity in the Marmara Sea region, NW Anatolia. J Geophys Res Solid Earth 12:27587–27601

Toscano MA, Peltier WR, Drummond R (2011) ICE-5G and ICE-6G models of postglacial relative sea-level history applied to the Holocene coral reef record of northeastern St Croix, U.S.V.I.: investigating the influence of rotational feedback on GIA processes at tropical latitudes. Quat Sci Rev 30:3032–3042

Tur H, Ecevitoğlu B (2000) Marmara Denizinin oluşumu ve Marmara Denizindeki aktif faylar. Uygulamalı Yerbilimleri Dergisi, n: 6 (in Turkish)

Vardar D (2006) Seismic stratigraphy of the Erdek Gulf and its vicinity. Istanbul University, Institute of Marine Science and Management, Istanbul, MSc Thesis (in Turkish)

Yaltırak C (2002) Tectonic evolution of the Marmara Sea and its surroundings. Mar Geol 190:493–529

Yaltırak C, Alpar B (2002a) Evolution of the middle strand of North Anatolian Fault and shallow seismic investigation of the south-eastern Marmara Sea (Gemlik Bay). Mar Geol 190:307–327

Yaltırak C, Alpar B (2002b) Kinematics and evolution of the Northern Branch of the North Anatolian Fault (Ganos Fault) between the Sea of Marmara and the Gulf of Saros. Mar Geol 190(1/2):351–366

Yaltırak C, Işler EB, Aksu AE, Hiscott RN (2012) Evolution of the Bababurnu Basin and shelf of the Biga Peninsula Western extension of the middle strand of the North Anatolian Fault Zone, Northeast Aegean Sea, Turkey. J Asian Earth Sci 57:103–119